UAV MONITORING OF DUNE DYNAMICS - ANNA BAY ENTRANCE, STOCKTON BIGHT

Nicolas Pucino[1][a], Sandro Condurso[2]

[1]University of Wollongong, NSW
[2]NSW-National Park and Wildlife Service - OEH, Nelson Bay
[a]Corresponding author: nicolas.pucino@hotmail.com

Introduction

"*When the causes and trends of coastal dune movement are well understood, tailored management strategies can be applied in order to maximize tourist attraction while maintaining a healthy and naturally dynamic geomorphic behaviour*" (Mitasova et al., 2005)
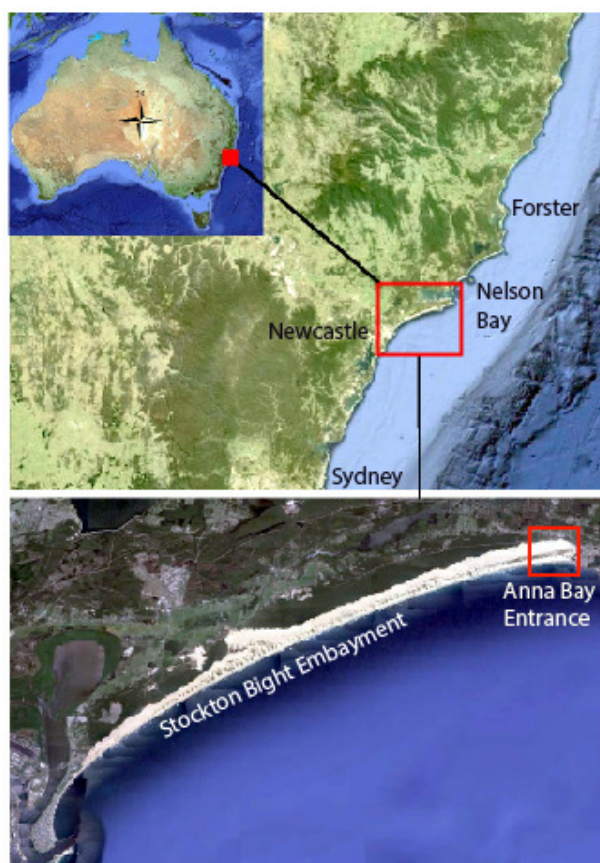

Figure 1 Location map of Stockton Bight

This site-specific (Anna Bay entrance) Unmanned Aerial Vehicle (UAV) survey and analysis is part of a broader environmental study conducted at the whole Stockton Bight (NSW) embayment scale. The full-study aims to understand Stockton Bight dune dynamics and migration trends, adding local knowledge to both managers, aboriginal community and visitors. Stockton Bight's management is challenged by its naturally dynamic geomorphic state, richness in aboriginal sites and artefacts, sand mining activities, high visitation and touristic impact. Its extent is a major issue to deal with. The study site, which is included in the Worimi National Park, features the southern hemisphere's largest mobile coastal sand mass (NPWS). With its 32 km, Stockton Bight is also the longest beach in NSW. Some of its transgressive dunes reach heights of 40m of elevation above sea level and its beach-backdune-transgressive dune system covers an area of 2700 ha, which means approximately 3800 football fields.

Given the aforementioned conditions, it is evident that the study of such a dynamic and geographically extended area implies trade-offs in spatial scales and analytical techniques.

Accordingly, this research features geospatial analysis of both LiDAR (whole-embayment analysis) and UAV (site-specific) digital terrain models. Upon deriving and mapping sand movement trends, the project will also explore sand mitigation measures for targeted locations to best achieve efficient and cost effective sand stabilisation outcomes.

The UAV solution at Anna Bay entrance

This conference paper describes methods and analysis of a topographical coastal surveys using UAV, Structure From Motion (SfM) and GIS, in Anna Bay entrance, the northern end of Stockton Bight (NSW, Australia) embayment. Here is the area where the most human pressure occurs as it is used as main northern entrance to the national park by tourists, locals, rangers, 4wd vehicles and every kind of recreational or touristic operator activities, including horse and camel riding, 4wd buses and trucks, sand boarding, dogs, etc. As the expected outcome in this area will be an effective and calibrated sand stabilisation strategy, beach morphodynamics and sand movements must be acknowledged and monitored. Thanks to the availability of an UAV system (SenseFly Ebee) and a fully certified, licensed and experienced surveyor (Condurso Sandro), very high spatial resolution (10cm) Digital Surface Models (DSM) and ultra-high (3cm) repetitive orthophotos have been generated and both volumetric change (cut and fill operation) and height differences (DSMs subtraction) analysed over time. These digital products are unevaluable to coastal monitoring projects, especially when the low time-step between acquisition dates allows seasonal variations to be observed. In fact, one of the major limitation of eolian geomorphology has been the relatively short temporal baseline of dune activity observations (Hugenholtz et al., 2012). To fully understand the changing morphology of a dune system, monthly or quaternarly surveys must be conducted in order to correlate data with storm events or weather patterns (Woolard and Colby, 2002; Andrews et al., 2002). Nowadays, UAV systems represent an extremely useful resource with endless potentials in topographic surveys of the coasts, capable of extending the analysis baseline at very short time-periods. This paper presents the details of the most recent UAV survey and the results of the geospatial analysis of all the available datasets (figure 2).

name	month	day	year	season	dsm	ortho	comment
20120903	9	3	2012	summer	y	y	no GCP
20140703	7	3	2014	winter	y	y	pilot_volume
20140905	9	5	2014	spring	n	y	foredune
20150515	5	15	2015	autumn	n	y	dsm corrupt
20150527	5	27	2015	autumn	y	y	pilot_volume
20151015	10	15	2015	spring	n	y	foredune
20151029	10	29	2015	spring	n	y	foredune
20151106	11	6	2015	spring	y	n	pilot_volume
20160317	3	17	2016	autumn	y	y	pilot_volume

Figure 2 Table of the available datasets. Only the datasets labelled as pilot_volume have been used for the geospatial analysis.

Structure from Motion

Thanks to the recent development of the so called "computer-vision approach", the fundamental principles that underpin a classic photogrammetric method are combined with robust and well documented image processing algorithms to create DSM models with sub decimetre accuracy, in a (semi) automated and user-friendly way. Classic aerial photogrammetry needs highly specialized personnel, expensive softwares and manned aircraft, perfectly calibrated and virtually distortion-free metric cameras, restrictive image collection requirements and long planning times. Structure from Motion (SfM) approaches allow non-specialized users to align and mosaic aerial photographs acquired

by consumer-grade medium resolution camera (though any camera can be potentially used) mounted on many different moving platforms ranging from balloons, UAVs and kites. In this research, aerial photography acquired with a surveyor grade UAV system has been processed with the classic SfM pipeline (figure 3). This consists in placing all the images acquired by the UAV aerial survey into a virtual terrain, aligning and stitching them together, correcting for distortions and georeferencing the mosaic (using Ground Control Points (GCPs) surveyed on the ground), identifying and extracting common features occurring in overlapping images, tying them together and finally computing the elevation of every pixel of the images.
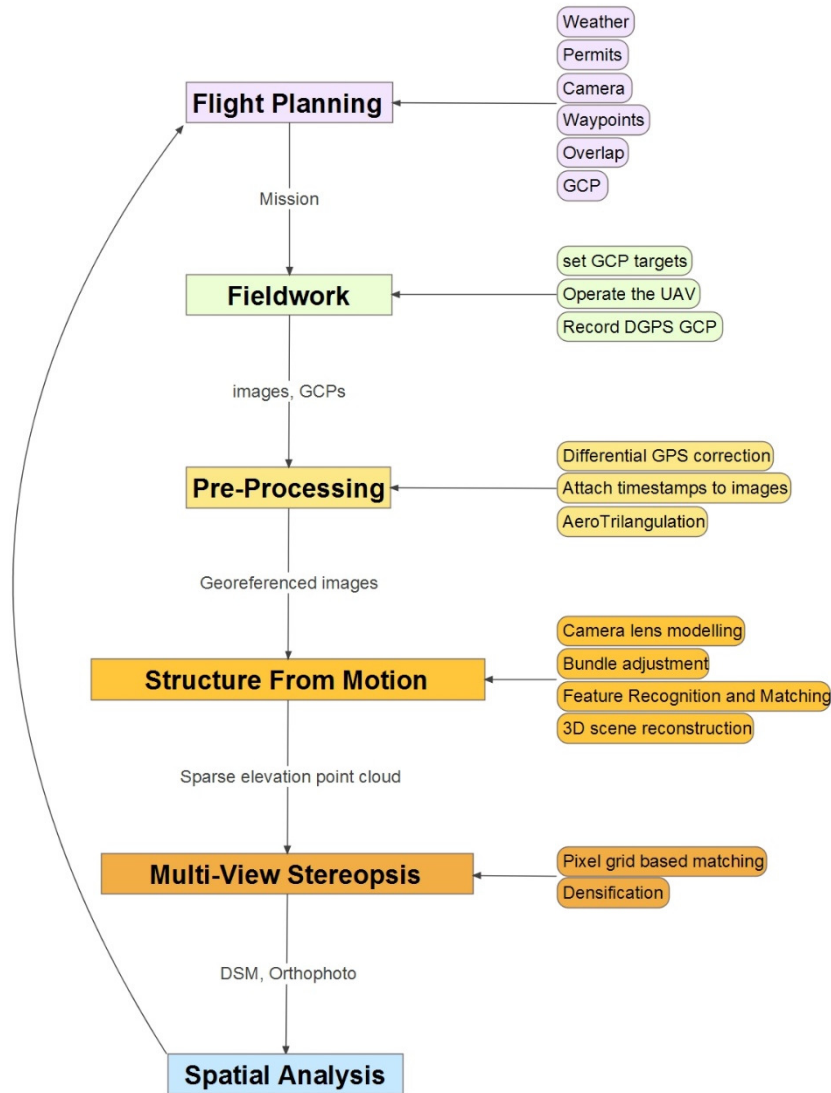

Figure 3 Scheme displaying the key steps used in most of the UAV SfM-related studies.

Drift Potentials

Monitoring dune activity means identifying, quantifying and interpreting dune surface changes related to the eolian sand transport potentials (Hugenholtz et al., 2012). In fact, dune activity is usually regarded as an index of eolian sand transport potential (Fryberger and Dean, 1979; Ash and Wasson, 1983; Lancaster, 1988). Amongst the different indices that exist in eolian geomorphology literature, the Fryberger method (Fryberger and Dean, 1979) for calculating sand Drift Potentials (DPs) and relate them to the wind energetic environment has been used in this study. Fryberger's method has been validated by many global sand sea (Fryberger and Dean, 1979; Wasson and Hyde, 1983; Bullard et al., 1996) and coastal studies (Miot da Silva and Hesp, 2010; Tsoar, 2005; Levin et al, 2014). The sand Drift Potential (DP) is a parameter that describes the maximum potential amount of sand that could be eroded and transported by wind coming from a determined direction over a period of time (Fryberger and Dean, 1979) and it is widely used all over the world and in Australia (Levin et al, 2014). DPs must be calculated in each of the wind direction component (12 or more Directional Classes; DCs). The assumptions are that the surface is composed by loose quartz grains (0.25-0.30 mm average diameter), no bedforms bigger than ripples are present, it is dry and clear of vegetation cover (Fryberger and Dean, 1979). It is calculated as

$$DP = \sum \frac{U^2(U - U_t)}{100} \times t$$

where U is the wind velocity (m/s, at 10m height from ground level) Ut is the threshold wind velocity (= 5 m/s) and t is the percentage of time that wind exceed Ut. Following the Belly method and valid for the aforementioned assumptions, a threshold velocity (Ut) of 5.97 m/s (11.6 knots) was adopted by Fryberg's global sand seas analysis. In Stockton Bight transverse dune environment, according to expert local geomorphologist (Thom et al. 1992) and in lack of in situ sand sample, the local threshold has been chosen at 5 m/s (9.72 knots). DPs from all the DCs can be resolved into the Resultant Drift Potential (RDP) and its direction as the Resultant Drift Direction (RDD) via a vector analysis. Following the original Fryberger's (1979) method sand roses can eventually be produced. Moreover, the RDP/DP is a measure of wind variability, used by Fryberger for classification depositional environments. The wind data utilised for the Fryberger's indexes have been collected by the Newcastle Nobby's Signal Station AWS, managed by the Bureau of the Meteorology (BoM). The station is situated at the southern end of Stockton Bight embayment, directly on the headland and facing the ocean. The station is at 33 m above mean sea level and 10m above ground, which is with the 10m assumption of Fryberger's method. The BoM wind measurements are designed to satisfy weather and climate monitoring needs. Its uncertainty tolerances are 10% of the wind speed when wind speeds are greater than 10 m/s and 1 m/s for wind speeds at or below 10 m/s.

Area of study

Stockton Bight transgressive sand barrier system (originally "Newcastle Bight", figure 1) is located on the coast of central New South Wales, Australia, between Port Stephens drowned river valley (north) and the mouth of the Hunter River at Newcastle. Stockton Bight embraces most of the features that characterise coastal NSW, namely, rocky headlands which compartmentalize an embayed and wave-dominated sandy beach or barrier, a steep and relatively narrow inner continental shelf and a limited supply of river sediment to the coast (Thom et al., 1992; Wright, 1996; Davies, 1974; Thom et al, 1981). The climate is temperate, providing minor seasonal variation around a mean warm and humid conditions. This climate highly increases the wave climate variability and sets a moderate to high-energy south-easterly swell (occasionally southerly). The tidal range is less than 2m (micro-tidal system). During the day, sea breezes dominate. Trade winds, swell and regional climate combined, result in the dynamisms that characterised the NSW beaches (Short, 1993). Anna Bay entrance geomorphology is dominated by (inland to seaside):

1) long-walled active ridge
2) mobile sand sheet of migrating transverse and barchanoid dunes (referred as "high dunes")
3) deflation plain
4) foredune
5) beach

Unfortunately, the UAV surveys do not cover the whole shore-normal transect from the long-walled ridge to the beach but only from the upper end of the deflation basin in contact with the transverse sand sheet to the swash zone. The deflation basin is shaped by the inland motion of the transgressive dunes. They migrate leaving behind an extensive and relatively deep basin, which lays parallel to the rear of the beach. The deflation basin is barely above the water table (which in Southeast Australia is very shallow) and is characterised by hummocky surfaces with low active dunes and vegetated patches. Transverse "high dunes" become more barchanoidal close to the deflation basin where the sand supply is limited. The seaward limit of the deflation basin is represented by the (currently) heavily dissected foredune system. The foredune is discontinued due to the occurrence of multiple blowouts. Blowouts are a specific eolian "dune-like" landform generated by holes along foredunes, wind erosion, sand deposition and trailing arms fixation by vegetation. These dunes are derived from the dissection of foredune by marine erosion, vegetation removal or human trampling. These blowouts channelize beach sediments through their arm, funnelling onshore winds that exacerbate erosion deepening its deflation basin and scouring its trailing arms. This process is known to be responsible of deposition of wind-borne sand behind the foredune, lowering the foredune and filling the deflation plain. The beach morphodynamics states that occur more often at Stockton Bight are those of the high-energy wave energy. Anna Bay is more exposed to SW swell and higher energy waves, resulting in dissipative, longshore bar and through and rhythmic bar and beach morphodynamic states. In general, this area experiences a wide spectrum of wave energy, the persistence of a longshore bar at the northern end of the embayment. In the SW end, the very coarse grainsize and the steeper beach face are more characteristic of reflective conditions, but purely reflective states are rare (Thom et al 1992).

Methods

In this section, the methods for the UAV survey, the DSM production (and accuracy) and the volumetric analysis are outlined.

The UAV survey and products accuracy

Here are reported the details of the last UAV survey, while the other UAV datasets had already been captured by Sandro Condurso, Park Systems Officer at the National Parks and Wildlife Service office in Nelson Bay (NSW).
This UAV survey took place the 17 March 2016 along the northern tip of Stockton Bight, covering the Anna Bay entrance in the Worimi National Park. It started early morning

Figure 4 Left: Differential GPS survey of GCPs. Right: eBee Sensefly with operator controller.

(7.00 AM), when weak coastal breezes and low sun elevation allowed stable flight and enhanced textural heterogeneity. The survey was divided in three distinct flights which have been subsequently merged in one single dataset. All the datasets were derived by a foam fixed-wing off-the-shelf SenseFly eBee, (figure 4) having an approximate weight of 0,69 kg, wingspan of 96 cm and an incorporated camera WX (6,170 X 4,627 mm sensor dimensions) of 18,2 MP.
According to the manufacturer, this aerial platform can fly for a maximum of 50 minutes with one standard 11,1 V (2150mAh) battery. However, this is only an indicative maximum value, as wind gusts require the UAV stabilisation manoeuvres depleting the battery at faster pace than in calm wind conditions. This UAV is able to withstand winds up to 12 m/s. Waypoints (see figure 5), speed, altitude (120 m above a.m.s.l, Australian maximum allowed) and lifting/landing areas were all calibrated and combined together (with eMotion software) for assuring a forward and side overlap of at least 80% between successive imageries along the flight path. The average Ground Sampling Distance (GSD) was 3,49 cm, the area covered in three missions was 222,76 ha (2,23 km2). The time spent for the fieldwork (UAV survey and Ground Control Points (GCP) differential GPS (dGPS) survey) was around 4h. Average flight times were 15 minutes, the greater part of the fieldwork being the dGPS survey. A total of 22 1X1, 5 m rectangular mats displaying an identification number and a cross (figure 4) were used as GCPs and regularly distributed across each of the three surveys area.
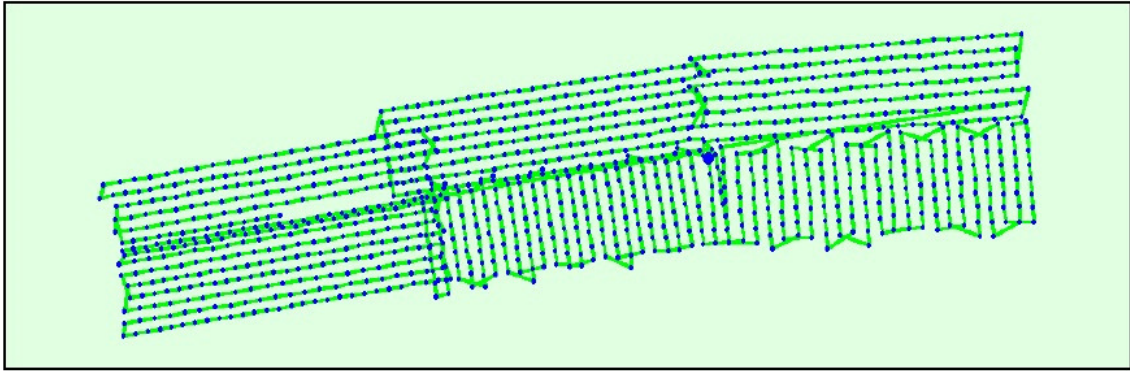
Figure 5 Waypoints and flight paths of the three flights merged together.

This GCP network is essential for Aero Triangulation (AT) and bundle block adjustments. Single frequency GNSS Trimble GeoXH receiver was used to collect GCPs's locations. For each GCP points, 3 minutes of static dGPS data was collected (1 point/s) and post-processed using Trimble® GPS Pathfinder® Office software. Correction data has been downloaded from CORSnet New South Wales's server for the two base stations the closest to the survey locations, which are Anna Bay and Newcastle East base stations.

Figure 6 Example of procedure of Aero Trinagulation performed by the operator within PostFLight Terra 3d. The same target on the ground is seen by different orientation and angles and the operator has to adjust the suggested points (by the software, using coarse on-board GPS coordinates) and place them in the centre of the X displayed by the targets. This will allows PostFlight Terra 3d to model the camera distortion parameters and perform SfM-MVS routine to extract DSM and orthophoto.

CORSnet-NSW is a network of permanent Global Navigation Satellite System (GNSS) tracking stations, which improve the accuracy of satellite positioning for users in NSW. According to the correction service provider (Trimble®VRS Now®) the horizontal accuracy achievable in optimal conditions with this type of differential correction is less than 2 cm. After code and carrier differential correction, the estimated accuracies for the GCPs locations improved from 3-5 m to 5-15 cm. However, based on past observations and local expertise of the surveyor, accuracies are believed to be in the order of 5 cm. After correction of the GCP points, an ASCII file is generated and opened into Postflight Terra 3d for AT (figure 6). The eMotion software is also used to attach the timestamps to each picture. In figure 6 is possible to see how the AT process is user-friendly and performed by visualising each target (in this case named 2_1), adjusting the suggested GCP XYZ coordinates (411170.207, 6372253.808, 3.925) by dragging the point to the centre of the "X" target. This will allow Structure from Motion and Multi-View Stereopsis to perform AT, bundle block adjustment, feature recognition and matching algorithms and more, in order to finally output the DSM and orthophoto. After AT, the post-processing phase can start. An Intel® Xeon ® CPU E5-2603 0 @ 1.80 GHz with 12 GB of RAM and NVIDIA Quadro 2000D (GPU) was used to process all the 1108 images

8

collected during the three surveys and merged together in a single dataset. The whole processing time (from AT to dense point cloud and mesh generation) was 23h. The median feature matches per calibrated image were 5324,07 (figure 7) and the georeferencing Root Mean Squared (RMS) errors were 0.019 m, 0.017 m and 0.006 m for the X,Y,Z coordinates respectively. The total positional RMS value is then 1.14 cm.
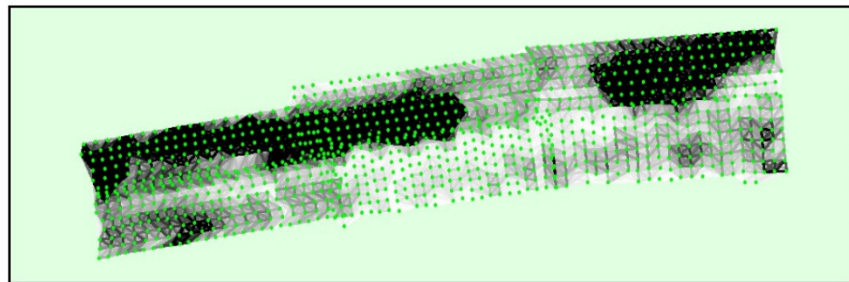

Figure 7 Number of matches and images focal points (green signs). Note how the lighter areas (less matchings) are located above the thin dune sheet of bare and deflated sand immediately behind the foredune, indicating high texture homogeneity, complicating the feature extraction and matching process.

The average elevation points spacing within the dense point cloud was 3.49 cm, varying according to the texture qualities of the location being sensed. Therefore, the final DSM was produced interpolating and re-gridding elevation points from the dense point cloud, yielding a final spatial resolution of 10 cm. The orthophoto pixel resolution however (figure 8) is of 3,5 cm.
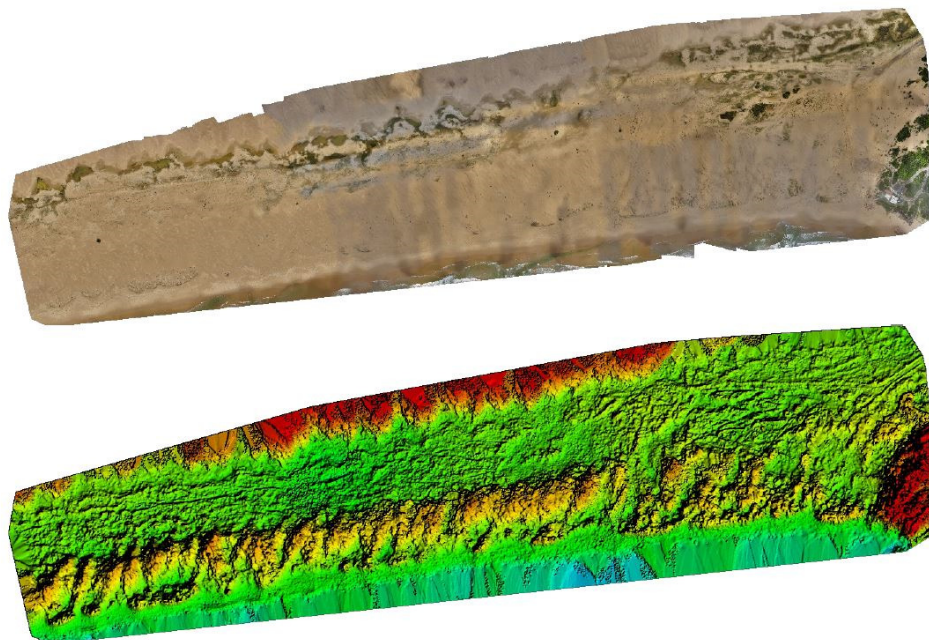

Figure 8 Orthophoto and sparse Digital Surface Model (DSM) before densification (MVS) of the surveyed area, as provided by the automatically generated accuracy report of PostFlight Terra 3d software.

All these digital products were generated using the GDA94/MGA zone 56 coordinate system, based on the Geocentric Datum of Australia 1994 (GDA94) and the Map Grid of

Australia 1994 (MGA94) and exported in common GIS file formats in order to be compatible with and further analysed by GIS platforms (ArcGIS 10.2, in this case).

The delineation of three discrete depositional environments was meant to offer a finer separation of volumes and differences during the analysis periods, providing insights on sediment dynamics in a cross-shore direction. Obviously, this is a simplification of the real sediment dynamics of this area, as longshore drift and lateral contributions to the shore-normal beach-foredune-deflation basin system are not taken into account. Moreover, UAV DSMs lack of the most important geomorphic feature of this system, which is the transverse dune system above the entrance. The high transverse dune sheet and especially the transgressive long walled ridge are supposed to be the sink of the whole Stockton Bight sediment compartment (Gordon and Roy, 1977). Thus, only general observations can be drawn from fine-scale volumetric changes in each of the sub-systems analysed. The delineation of the three sedimentary compartments has been based on visual interpretation of orthophoto (where available) and three shore-normal elevation profiles traced from the landward limit of the study area to the seaward one, in each dataset. In figures 9, 10, 11 and 12 it is possible to see how this process works, resulting in the final sub-compartmentalisation (figure 13).
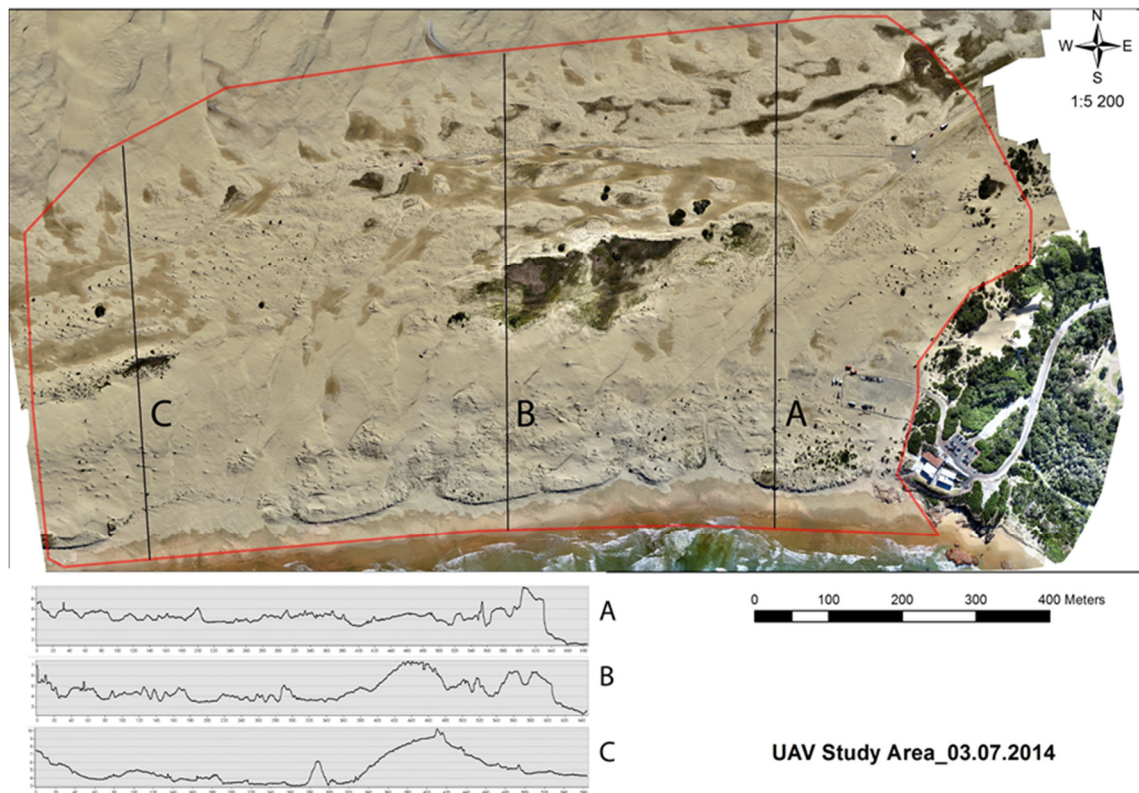

Figure 9 Orthophoto and elevation profiles used to separate the study area in the three sub-systems (beach-foredune-deflation basin). Date of data acquisition: 03.07.2014.
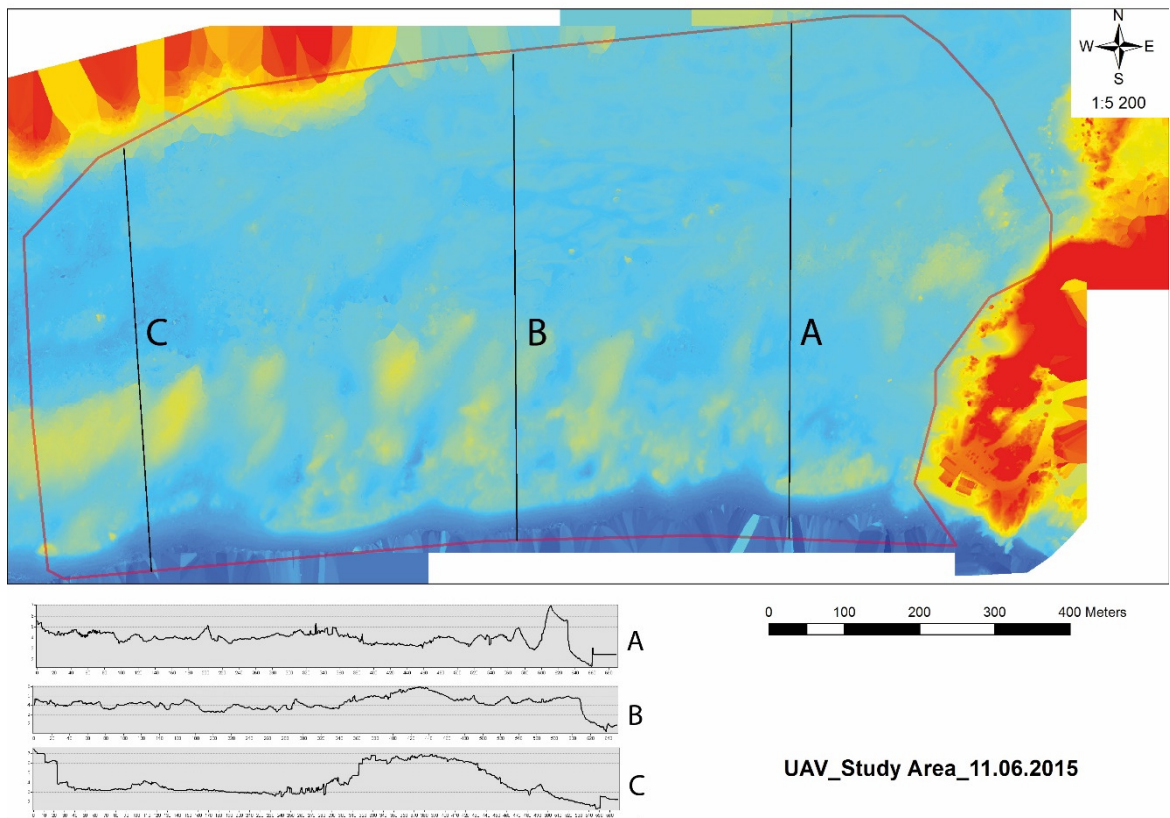
Figure 10 In this case, the DSM was available while the orthophoto was not. Only the elevation profiles were used for interpretation. Date of data acquisition: 11.06.2015.
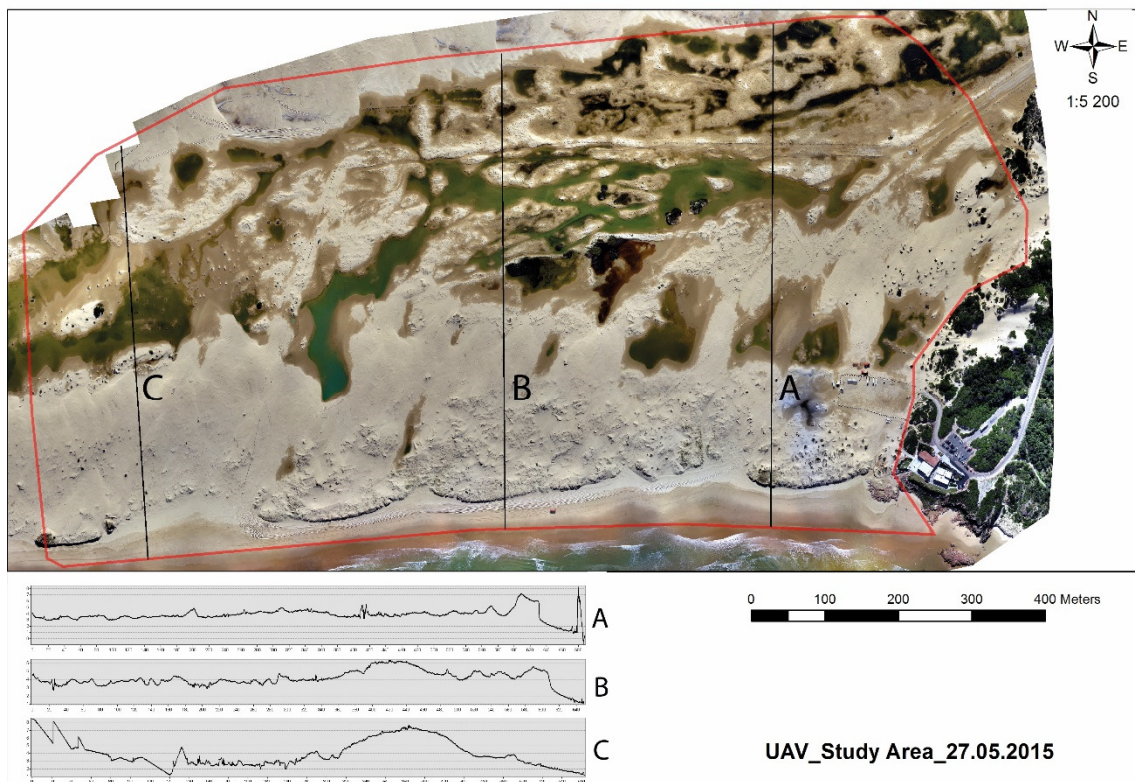

Figure 11 Orthophoto and elevation profiles used to separate the study area in the three sub-systems (beach-foredune-deflation basin). Date of data acquisition: 27.05.2015.
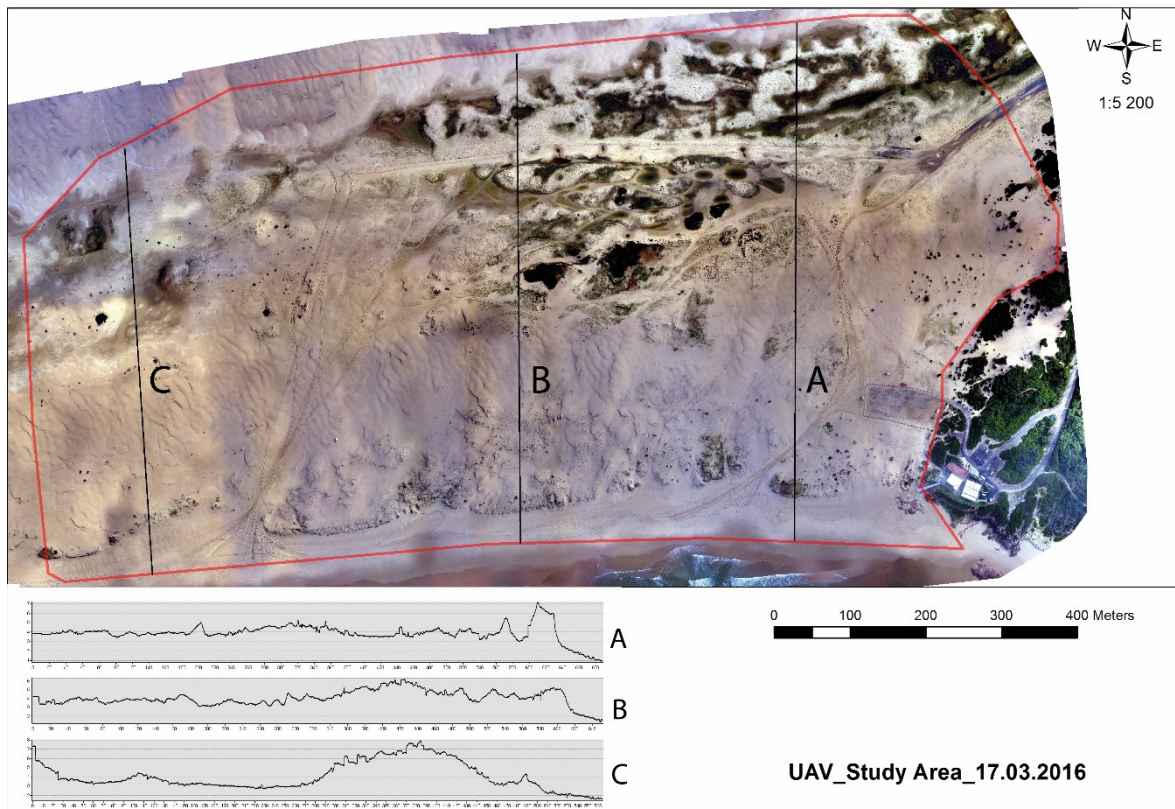
Figure 12 Orthophoto and elevation profiles used to separate the study area in the three sub-systems (beach-foredune-deflation basin). Date of data acquisition: 17.03.2016.

Please note that the foredune looks abnormally protruded landward because of the inclusion of the thin and bare sand sheet formed by deflated sediment eroded from and transported over the foredune-beach system. Once the sub-systems have been identified, volume and height differences can be calculated by running the Cut and Fill algorithm (volume) or simply by subtracting the most recent DSM from the earlier one
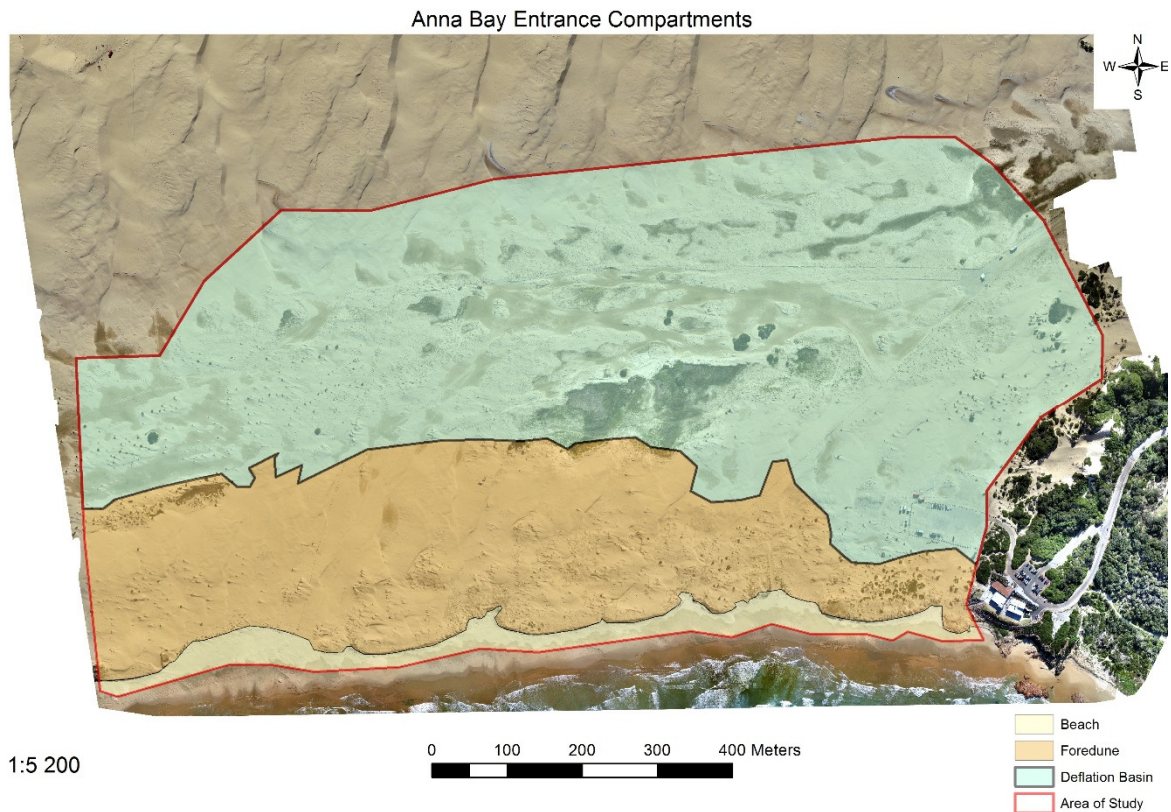
Figure 13 The discrimination of the study area (red boundary) in three distinct but inter-connected sub-systems, namely the beach, the foredune and the deflation basin.

(height). By using the Cut and Fill tool in ArcMap 10.2, an output raster is returned with cell values having as attribute the volumetric difference from raster 1 to raster 2. Therefore, positive volume cells (displayed in blue) are where sediment was cut (erosion), and negative ones (displayed in red) indicate where sediment was filled (accretion). Those accretion and erosion cells have been grouped based on the sub-systems they occur and then summed up to calculate volume change.

Results and Discussion

The following pages provide images (figures 14-17) of the results of the volumetric/height analysis for every time period. The relative data tables and discussion are provided at the end of the following pages.
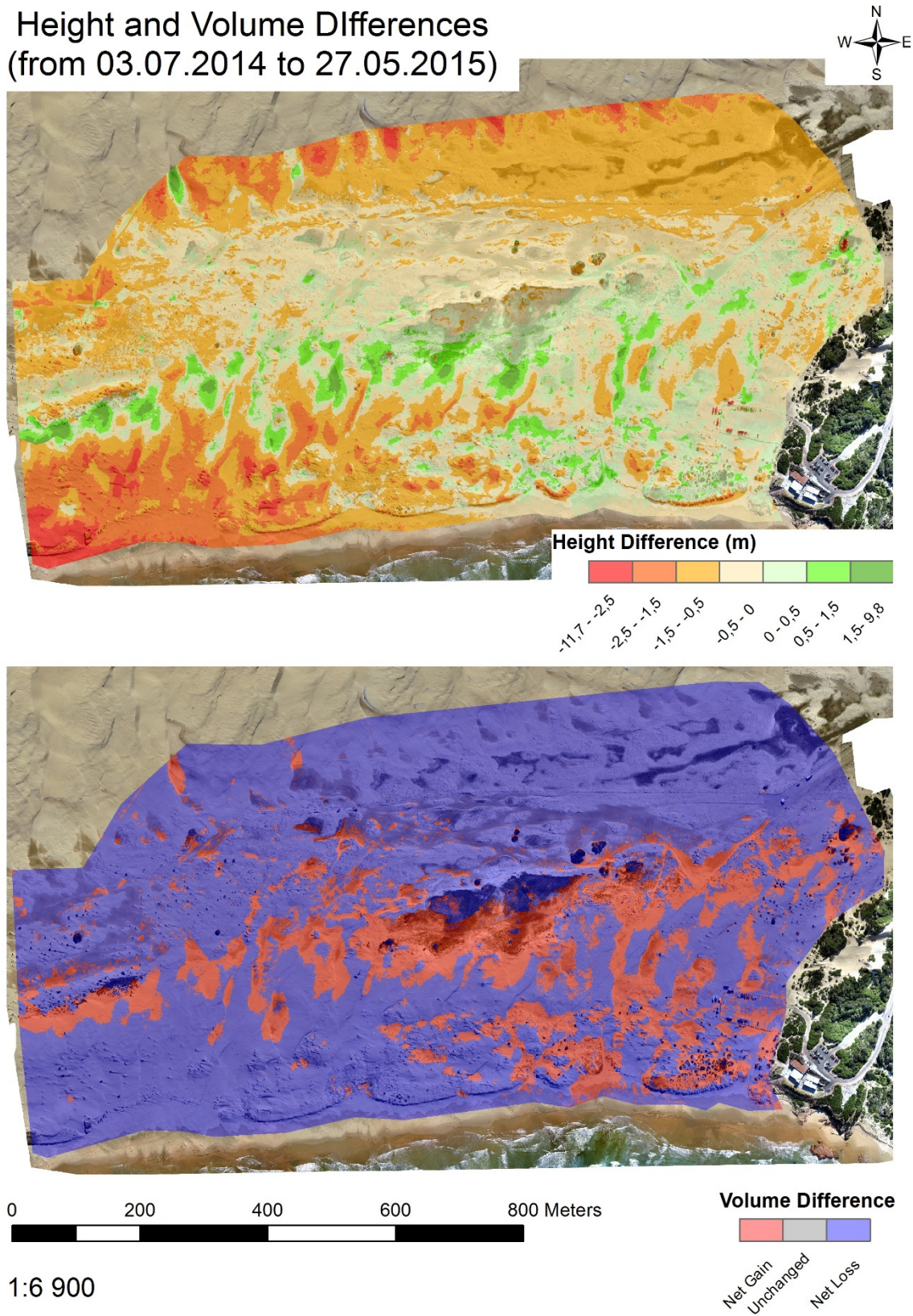

Figure 14 Height and volume difference maps of voldiff_1 period.

Height and Volume DIfferences
(from 27.05.2015 to 11.06.2015)

Height Difference (m)

-11,7 - -2,5 | -2,5 - -1,5 | -1,5 - -0,5 | -0,5 - 0 | 0 - 0,5 | 0,5 - 1,5 | 1,5- 9,8

0   200   400   600   800 Meters
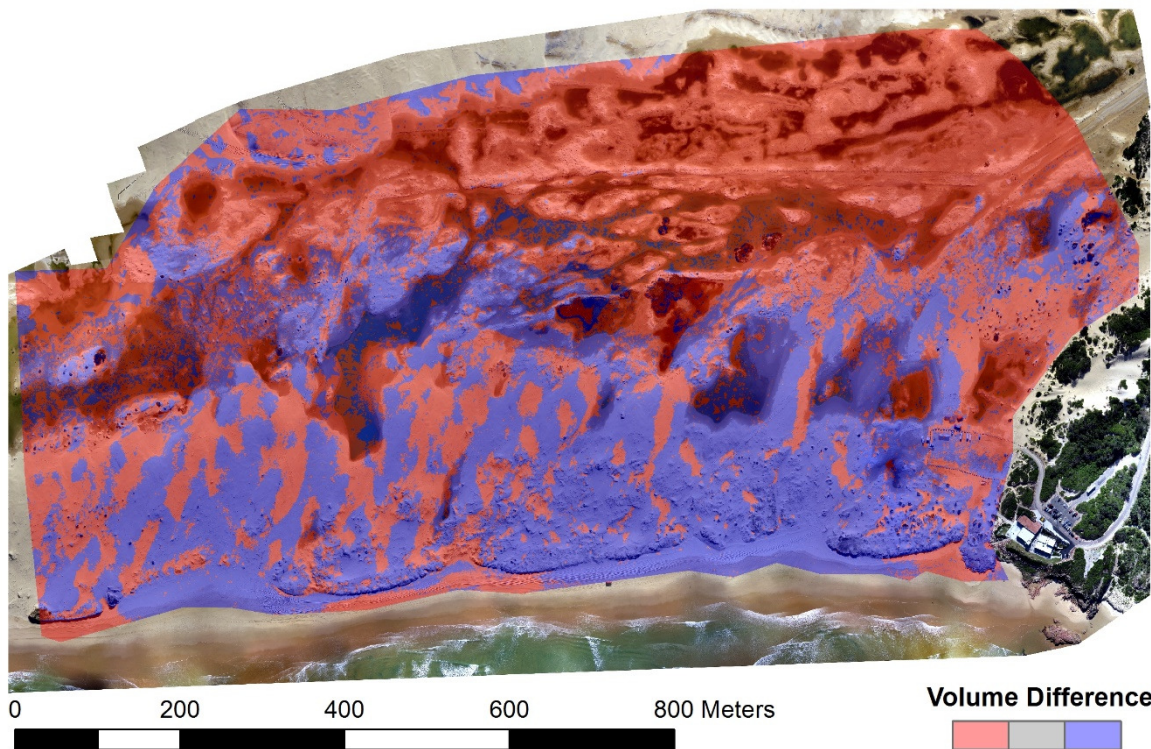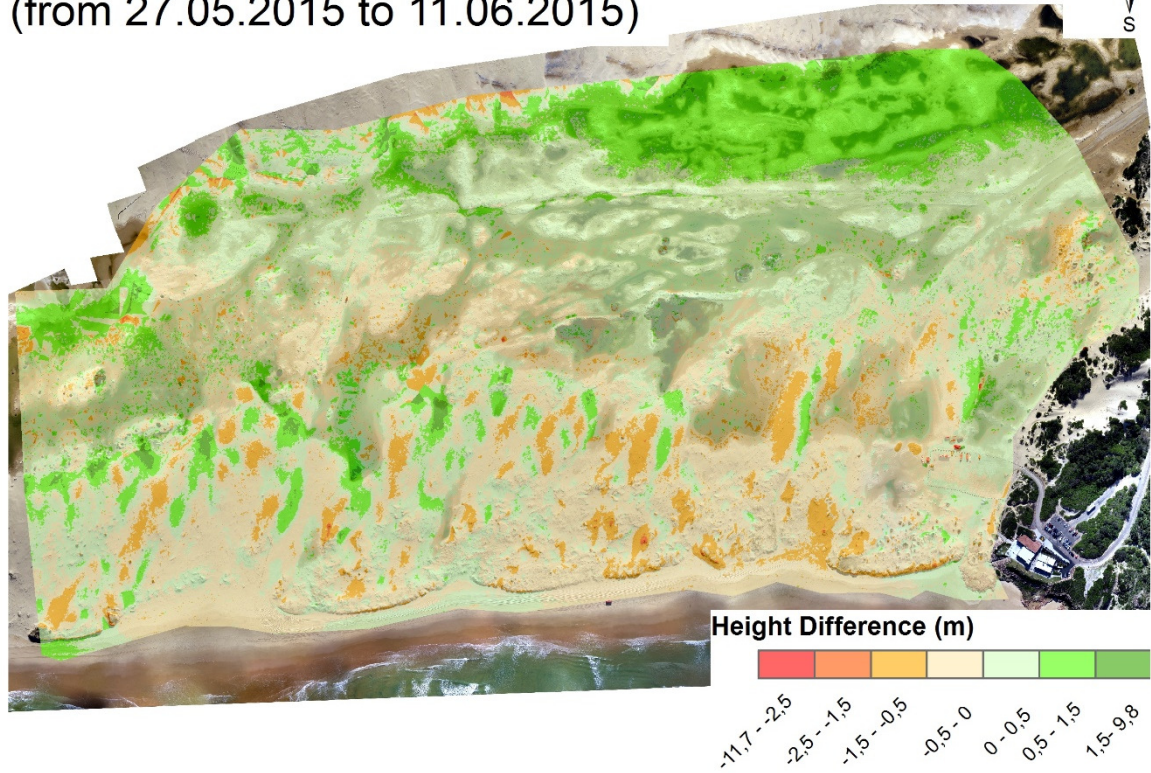
1:6 900

Volume Difference

Net Gain   Unchanged   Net Loss

Figure 15 Height and volume difference maps of voldiff_2 period.

Height and Volume DIfferences
(from 11.06.2015 to 17.03.2016)

N
W E
S

Height Difference (m)

-11,7 - -2,5　-2,5 - -1,5　-1,5 - -0,5　-0,5 - 0　0 - 0,5　0,5 - 1,5　1,5 - 9,8

0　200　400　600　800 Meters

1:6 900

Volume Difference

Net Gain　Unchanged　Net Loss
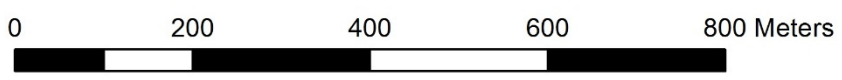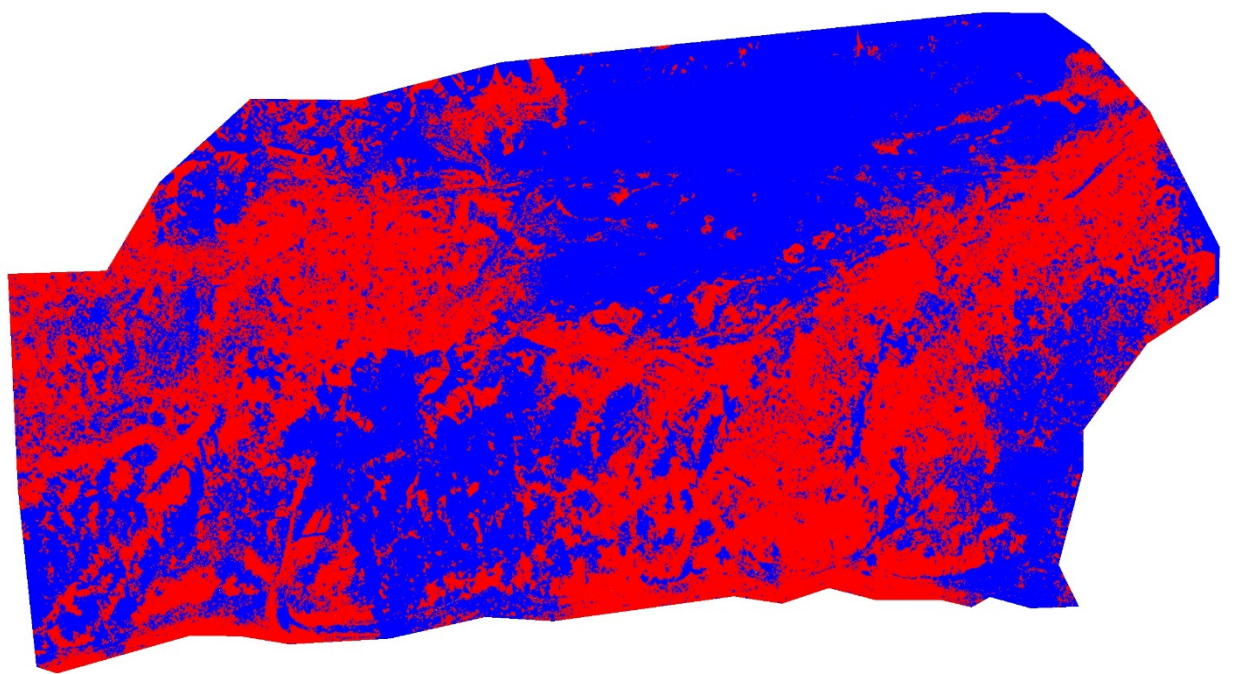
Figure 16 Height and volume difference maps of voldiff_3 period.

Height and Volume Differences (from 03.07.2014 to 17.03.2016)

Height Difference (m)

-11,7 - -2,5 | -2,5 - -1,5 | -1,5 - -0,5 | -0,5 - 0 | 0 - 0,5 | 0,5 - 1,5 | 1,5 - 9,8

0   200   400   600   800 Meters

1:6 900

Volume Difference

Net Gain | Unchanged | Net Loss
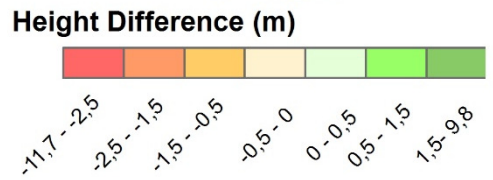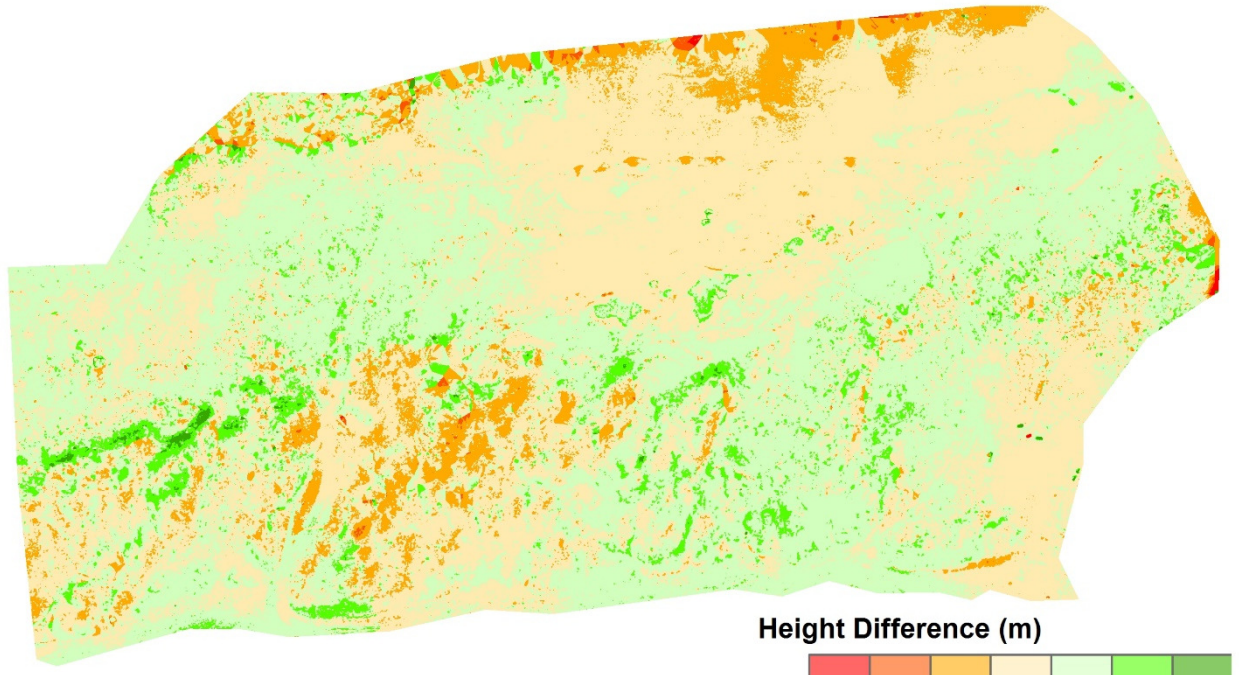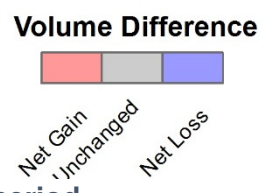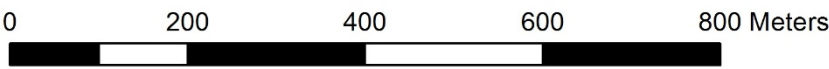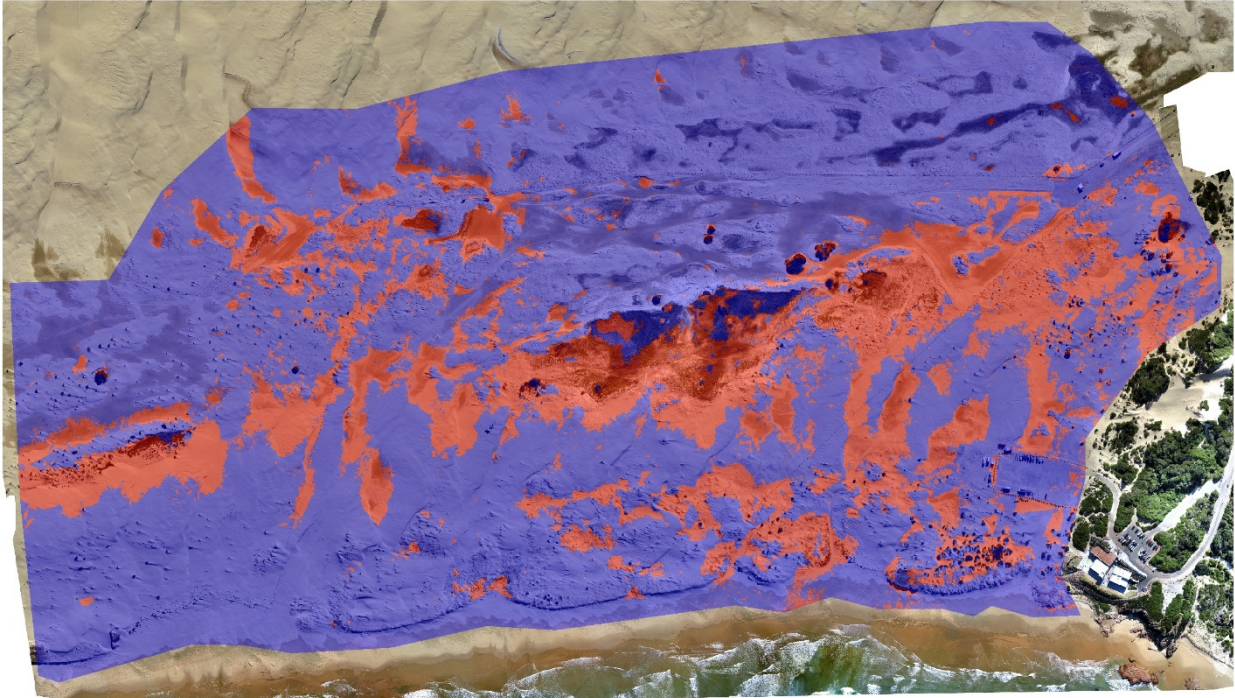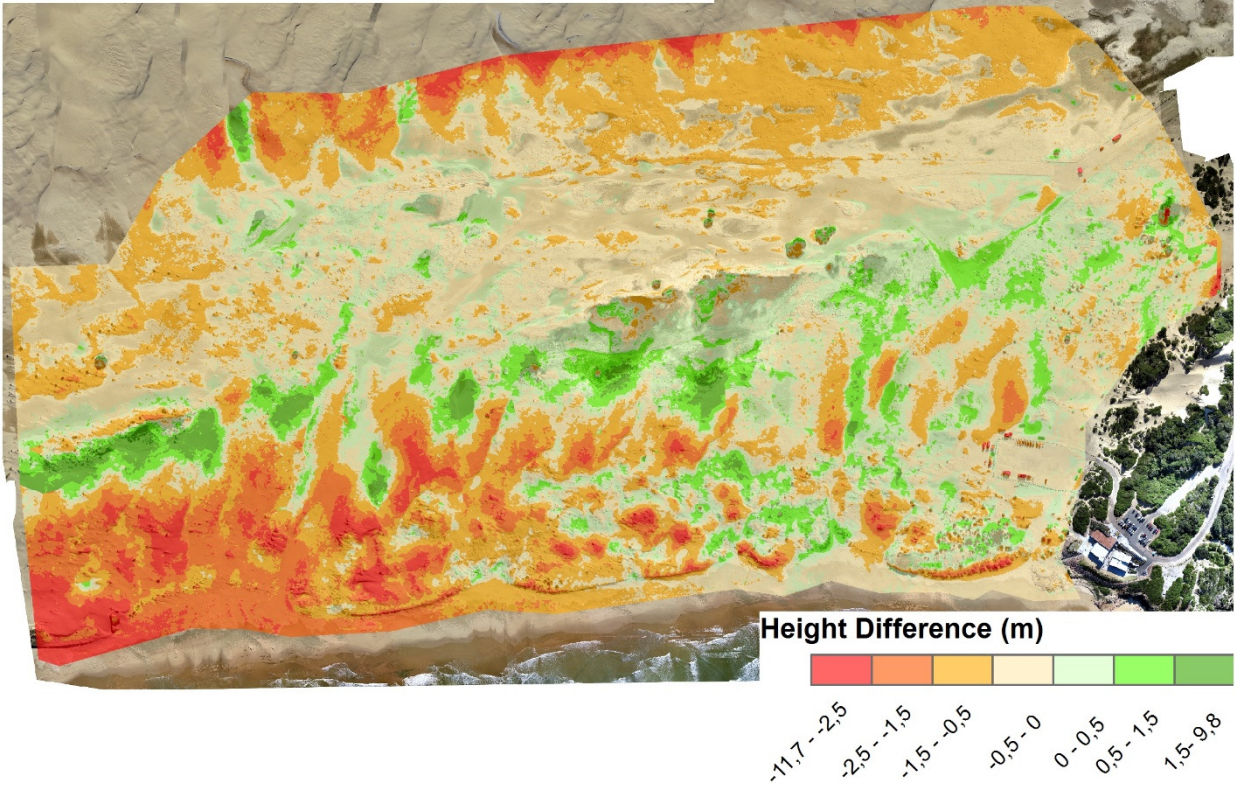
Figure 17 Height and volume difference maps of voldiff_long period.

voldiff1	accretion	erosion	net
beach	868,61964	40890,897	-40022,3
foredune	34964,931	190046,34	-155081
deflation basin	29633,456	252492,66	-222859
tot	65467,007	483429,9	-417963

The first period (voldiff_1) represents almost one year (328 days) of time interval and it is characterised by the highest net loss of all the periods (- 417'963 m3). The deflation basin has been the sub-system with the largest net sediment loss (- 222'859 m3) followed by the foredune (- 155'081 m3) and the beach (-40'022 m3). By looking at detailed sub-systems erosion/accretion values, it is interesting to note how there is a moderately high accordance with a dominance in the shore-normal sediment transportation. The loss of the beach (- 40'891 m3) is close to the foredune sediment accretion (+ 34'965 m3), with only 5'926 m3 of difference which could be the lateral contribution from outside the system. However, the foredune sub-system loss (- 190'046 m3) is much higher than the deflation basin accretion (+ 29'633 m3), suggesting that 160'413 m3 of foredune sediment has not contributed to the deflation basin infilling and it has exited the system or partially contributed to beach accretion.

Figure 14 clearly shows the general sediment loss of the beach and evidences how the only accretion areas are located above the rocky headland that tops up the embayment or at the foredune dissections (blowouts) used as entrances by 4WD, touristic operators and all kind of beach users. The foredune sub-system accreted only at its northern end, where vegetation increases surface roughness, reducing the surface wind and facilitating sedimentation. Interestingly, the border between foredune sub-system and deflation plain is where the majority of the accretion occurred, showing how the upper part of the deflation basin and the partial transverse dunes have lost sediment in favour of that area. From the height map, it is possible to note how the areas of most height loss or gain can track the barchanoid ridges and individual barchans migration paths. Please remember that the background orthophoto is always the initial state (in this case captured on 3 July 2014). By observing contiguous reddish (height loss) and greenish (height gain) area is possible to infer that these dunes migrated predominantly toward the NNE-NE and these observations are validated by the sand drift potential analysis. In fact, this period was characterised by a high wind energy (872 VU) coupled with an unusual high wind variability index (0, 67), which means that a less complex effective wind regime occurred. This resulted in a very high resultant sand drift potential (RDP) of 584 VU toward the NNE (RDD = 35°).

voldiff2	accretion	erosion	net
beach	2082,3582	5968,643	-3886,28
foredune	33247,733	46807,876	-13560,1
deflation basin	140250,46	34172,47	106078
tot	175580,55	86948,989	88631,56

The second period (voldiff_2) represents a 5 months interval (163 days) and shows a net accretion of + 88'869 m3 in the system due to the impressive net infilling of the deflation basin of + 106'078 m3. A positive gradient in accretion amounts is observed, increasing from the beach (+ 2'082 m3), the foredune (+ 33'248 m3) up to the deflation basin (+ 140'250 m3). This time, the shore-normal sediment transportation is less dominant than the previous period. The foredune accretion volume was well above (27'279 m3 of difference) the beach erosion one (- 5'969 m3). There is also a large difference of 93'442 m3 of sediment between the foredune sediment loss (- 46'808 m3) and the deflation basin accretion. Hence, this period could be dominated by a strong lateral contribution or a "reversed" trend with respect to the precedent one, with sand

being transported from the deflation plain (perhaps the high transverse dune sheet?) toward the beach. When the spatial distribution of loss/gain areas displayed in figure 15 are taken into account, it is evident how the majority of the sediment gain areas are located in the upper part of the deflation basin, which is in contact with the high dunes. The "reversed" hypothesis could be retained only if sediments are entering the deflation plain sub-system from the high transverse dunes. The foredune system shows a pattern of elongated accumulation/erosion areas, which suggests that sand has moved in a NE-E direction. The height map better evidences how is especially the barchanoid sand sheet that migrates NE-E, while the seaward margin of the foredune sub-system features a general loss except localised accretions at the southern blowouts and at the northern rocky headland. According to the wind data of this period, the resultant sand drift was low (RDP = 51 VU) toward NNE (RDD = 25°) due to the overall effective wind energy was intermediate (DP= 216 VU) further attenuated by a fairly complex wind regime (RDP/DP = 0, 25).

voldiff3	accretion	erosion	net
beach	4776,6796	1748,9882	3027,691
foredune	33146,635	39491,419	-6344,78
deflation basin	49214,387	70839,216	-21624,8
tot	87137,702	112079,62	-24941,9

The third period (voldiff_3) includes 132 days and shows a net loss of - 24'942 m3 of sediment from the system. Interestingly, a net beach accretion (+ 3'028 m3) has been observed in spite of the general erosional trend, especially marked within the deflation basin sub-system (- 70'839 m3). The shore-normal sediment transportation is fairly poor, once again, probably due to the lateral contribution, which comes from outside the system. There is a significantly large difference of 31'398 m3 of sediment between beach erosion (- 1'749 m3) and foredune accretion (+ 33'147 m3). This shows how a significant amount of sediment has entered the foredune sub-system from outside the system or the deflation basin. The difference between foredune erosion (- 39'491 m3) and deflation basin infilling (+ 49'214 m3) of 9'723 m3 is relatively lower and shows how the deflation basin lateral (or high transverse dune sheet) contribution are relatively less important. Regarding the spatial distribution of gain/loss areas within specific sub-systems, no orthophoto was available to compare the prior-change environmental situation with the mapped volumetric and height changes. Spatial patterns by visual inspection of figure 16 are not as evident as previous periods. However, it can be observed that the beach accretion occurred all over the sweep area except in some isolated locations. Interestingly, this is the only time that no accumulation has been recorded at the rocky northern end of the study area. The foredune, immediately behind the beach, appears to be eroded at its top and accreted just few meters landward. This "flattening" is particularly appreciable in the height map, where orange areas showing height decrease are mainly found on the top of the foredune and are often flacked by a landward green area, showing height increase. The upper foredune subsystem (barchanoid sand sheet) concentrates its volumetric loss in its western part. The central part is characterized by accumulation while the far east (next to the headland) displays net sediment loss. From this configuration seems that sediments have entered the foredune sub-system by the west. The deflation basin loss is focused on its northern and north-eastern part. It is difficult to infer sand movement directions from figure 16 and can only be modelled by using sand drift potential analysis. During this time period, a low (RDP= 93 VU) northern (RDD= 6°) sand drift has to be expected. The overall wind energy was intermediate (DP = 252 VU) with a simple wind regime (RDP/DP = 0, 37).

voldifflong	accretion	erosion	net
beach	721,8645	41603,446	-40881,6
foredune	49886,681	224872,93	-174986
deflation basin	48165,791	186560,79	-138395
tot	98774,336	453037,17	-354263

When the period from the earliest UAV survey to the latest (voldiff_long, 623 days) is taken into account, the very short-term variability observed might not be so evident, but it is important to remember that these types of surveys are only temporal snapshots of the environmental conditions that were present at the time of every UAV survey. This means that the longer period might reflect an apparently stable situation because of tremendous variability in inter-compartment sediment exchanges that have occurred from the first to the last UAV survey. Thus, volumetric changes calculated in this longer period hide the oscillations that are so important to depict for effective sand stabilisation solutions. Thus, the more surveys are operated in short time intervals the more precise the volumetric changes can be captured and reliable solutions can be proposed. Keeping in mind the aforementioned considerations, voldiff_long displays a behaviour similar to voldiff_1. A relatively very high net loss occurred (-354'263 m3) in the system. Interestingly, the foredune sub-system is the most eroded one (174'986 m3) followed by the deflation basin (138'395 m3) and the beach lost the same amount (-40'881 m3) of sediment as during voldiff_1 (-40'022 m3). While there are only 8'284 m3 of difference between beach erosion and foredune accretion (49'887 m3), the difference between foredune erosion and deflation basin accretion (48'166 m3) is remarkably high, showing that 176'707 m3 of sediment has been lost from the foredune and not stored within the boundaries of the deflation basin. By looking at the maps (figure 17), a very similar situation to voldiff_1 is observed, showing how in the longer term landward cross-shore sediment transportation dominates Anna Bay entrance.

Conclusion

UAV surveys and fine-scale site-specific analysis revealed useful to identify these sand movement trends and volumetric interchanges between sub-systems. The results highlight how shorter periods evidence western influx of sediment while yearly and bi-yearly periods suggest that landward cross-shore sediment transport is dominant, which comes from the beach (across blowouts) and from the erosion of the foredune. Generally, the stabilization works imply sand fencing traps, avoidance of littoral erosion during storms, provision of sand source for seasonal changes in beach slopes and plantation of native vegetation communities (Navarro et al., 2011).
Hence, two different type of interventions are needed in order to mitigate both short and long-term sand drift. The first intervention is the mechanical stabilisation of the deflated sand sheet behind the eroded foredune. Mulch, which is locally available, can be used for covering this area uniformly, preventing saltation and decreasing surface wind velocity. After the mechanical stabilization, planting trees and perennial vegetation will permanently stabilise the deflated sand sheet. During this phase, a soil and local vegetation expert must be contacted in order to determine:

1) The best planting period and specimens
2) The optimal density of planting
3) How the ground should be preparation for hosting the rooting system and facilitates the water retention
4) The optimal planting strategy

The second intervention aims to stop short-term pulses of migrating sand coming from the west, as observed from UAV sand movement analysis. This can be achieved by

stimulating the creation of an *ad-hoc* dune, which will be oriented normal to the prevailing RDD.

Interestingly, these two major interventions could be simultaneously accomplished by applying the so-called "*aerodynamic method*". This method uses the wind's speed to convoy unwanted sand toward a different direction than the prevailing effective wind direction. This is possible by placing fences at an angle of 120° to 140° to the RDD. In this way, obstacles in the path of the transporting wind deviates and accelerates the air flow, eroding the unwanted sand and building it up in another location. It is important not to generate any turbulence. Thus, the preliminary idea is to protect the road in its southern trait when it crosses the barchanoid sand sheet by creating a shield dune, which in turn convoys sediment toward the hummocky foredune previously mechanically stabilised increasing its accretion rate.

To sum up, to contrast the local sand drift, the following actions should be considered:

1) Accretion and stabilisation of dunes (referred as "shield dunes") located at the western side of the thin barchanoid sand sheet to contrast the short term western sand drift
2) Foredune backdune stabilisation and blowouts recovery to contrast the shore-normal sand transport
3) Foredune and shield dunes have to be fenced to prevent human trampling and possible re-activation

However, this is only a hypothetic solution that needs to be carefully assessed before any decision can be taken. Effectiveness in the long term of sand fencing still has to be evaluated by continuous monitoring. Another issue that might arise is related to the foredune vegetalisation process. In fact, if the sediment flux supplied by the aerodynamic divergence of the shield dune is excessively high, then vegetation development might be challenged. In addition, blowouts need to be sealed in order to avoid onshore winds to funnel thru them and activating freshly sand deposits provided by this mechanism.

References

- Andrews, B., Gares, P.A., Colby, J.D., 2002. Techniques for GIS modelling of coastal dunes. Geomorphology 48, 289–308.
- Ash, J. E., & Wasson, R. J. (1983). Vegetation and sand mobility in the Australian desert dunefield. *Zeitschrift fur Geomorphologie*, *45*(Supplement), 7-25.
- Bullard JE (1997) A note on the use of the "Fryberger method" for evaluating potential sand transport by wind. J Sediment Res 67: 499–501
- Davies, J.L., 1974. The coastal sediment compartment. Australian Geographical Studies 12, 139–151. doi:10.1111/j.1467-8470.1974.tb00270.x
- Fryberger, S. G., & Dean, G. (1979). Dune forms and wind regime. *A study of global sand seas*, *1052*, 137-169.
- Gordon, A.D., Roy, P.S., others, 1977. Sand movements in Newcastle Bight, in: Third Australian Conference on Coastal and Ocean Engineering, 1977: The Coast, the Ocean and Man, The. Institution of Engineers, Australia, p. 60.
- Hugenholtz, C.H., Levin, N., Barchyn, T.E., Baddock, M.C., 2012. Remote sensing and spatial analysis of aeolian sand dunes: A review and outlook. Earth-Science Reviews 111, 319–334. doi:10.1016/j.earscirev.2011.11.006
- Lancaster, N., 1988. Development of linear dunes in the southwestern Kalahari, southern Africa. Journal of Arid Environments 14, 233–244.
- Levin, N., Neil, D., & Syktus, J. (2014). Spatial variability of dune form on Moreton Island, Australia, and its correspondence with wind regime derived from observing stations and reanalyses. *Aeolian Research*, *15*, 289-300.

- Miot da Silva, G., Hesp, P., 2010. Coastline orientation, aeolian sediment transport and foredune and dunefield dynamics of Moçambique Beach, Southern Brazil. Geomorphology 120, 258–278. doi:10.1016/j.geomorph.2010.03.039
- Mitasova, H., Overton, M., Harmon, R.S., 2005. Geospatial analysis of a coastal sand dune field evolution: Jockey's Ridge, North Carolina. Geomorphology 72, 204–221. doi:10.1016/j.geomorph.2005.06.001
- Navarro, M., Muñoz-Pérez, J.J., Román-Sierra, J., Tsoar, H., Rodríguez, I., Gómez-Pina, G., 2011. Assessment of highly active dune mobility in the medium, short and very short term. Geomorphology 129, 14–28. doi:10.1016/j.geomorph.2011.01.009
- NPWS- NSW National Parks and Wildlife Service | Home [WWW Document], n.d. . NSW National Parks. URL http://www.nationalparks.nsw.gov.au/ (accessed 5.28.16).
- Short, A. D. (1993). Beaches of the New South Wales Coast. *Australian Beach Safety and Management Program, Sydney*.
- Thom, B. G., & Thom, B. G. (1992). Coastal geomorphology and quaternary geology of the Port Stephens-Myall Lakes area.
- Thom, B. G., Bowman, G. M., & Roy, P. S. (1981). Late Quaternary evolution of coastal sand barriers, Port Stephens-Myall Lakes area, central New South Wales, Australia. *Quaternary Research*, *15*(3), 345-364.
- Tsoar, H., 2005. Sand dunes mobility and stability in relation to climate. Physica A: Statistical Mechanics and its Applications 357 (1), 50–56.
- Wasson RJ, Hyde R (1983) Factors determining desert dune type. Nature 304:337–339
- Woolard, J.W., Colby, J.D., 2002. Spatial characterization, resolution, and volumetric change of coastal dunes using airborne LIDAR: Cape Hatteras, North Carolina. Geomorphology 48, 269–287.